NASA Contractor Report 181788

Noise Produced by Turbulent Flow Into a Rotor: Theory Manual for Noise Calculation

R. K. Amiet

United Technologies Research Center
East Hartford, CT

NASA

National Aeronautics and
Space Administration

Langley Research Center
Hampton, Virginia 23665-5225

TABLE OF CONTENTS

INTRODUCTION

The present report gives a detailed description of a computer program for the calculation of the noise produced by a rotor encountering a turbulent flow field. This represents the final product of an extended research effort on this subject, beginning with a theoretical study of the leading edge noise produced by an airfoil moving through turbulence[1]. Comparison with experimental and further theory was given by Paterson and Amiet[2]. A more detailed examination of the effects of varying the various parameters in the theoretical calculation is given in reference 3.

This computer program is critically dependent on the availability of relatively simple airfoil response functions that include the effects of compressibility and skewed gusts.These are given in references 4-8; only the necessary relations are presented here. Also needed is a turbulence model; that used initially was the Karman spectrum which can be found in many texts such as reference 9. This has more recently been extended, as discussed below.

This initial analysis was applicable to the case of the rectilinear motion of an airfoil. Using the principles elaborated in references 10 and 11, the analysis was extended in reference 12 to the case of rotary motion of an airfoil such as that of a propeller or helicopter rotor. This is based on an integration of "instantaneous spectra" around the azimuth, and includes retarded time effects on the generating source as discussed, for example, in reference 13.

The analysis of reference 12 is not limited to isotropic turbulence; in principle, any arbitrary turbulence spectrum can be specified. Because of lack of a good non-isotropic model, however, the computer program was initially written assuming an isotropic turbulence. The present program extends this by allowing a particular type of non-isotropic turbulence. In particular, the turbulent spectrum input to the program is assumed to be produced by an isotropic turbulence that has undergone a rapid contraction. The spectrum is calculated by the analysis of reference 14 (together with the program noted in the following paragraph for calculation of the deformation tensor). This is a minor extension of the classical analysis of Ribner and Tucker[15] in which is calculated the spectrum of turbulence undergoing a rapid contraction. This analysis is based on the concept that the turbulence is composed of vorticity, behaving purely kinematically and moving with the local fluid velocity. The final vorticity distribution, and thus, the velocity spectrum, can then be determined using the classical equations of Cauchy[16] for the distortion of vorticity by a deformation.

The present program does not calculate the fluid deformation that is necessary to complete the turbulence definition. The extension of the present program to include the non-isotropic case was developed in conjunction with a fluid deformation analysis of Simonich. This is a mean flow calculation that replaces the rotor and its wake by a series of vortex rings to simulate the flow field induced by the rotor tip vortices. Further details of this analysis and calculations showing the use of the two programs together are given in reference 17. The two programs can be used independently, but the deformation program, also available as an ANOPP module, is intended to be used in conjunction with the present noise prediction program. If this is desired, the ANOPP theory manual describing the deformation program (the companion to the present theory manual), should also be consulted. The programs have been configured so that the output of the deformation program is directed as input to the present noise prediction program.

The present program can also be run independently. For example, an isotropic turbulence can be assumed; the deformation tensor input is then the identity matrix (the diagonal matrix with 1's on the diagonal). The program can also be independently run with any arbitrary deformation that the user wishes to specify. This allows the user to investigate the effect of the any particular deformation tensor on the noise.

1

ANALYSIS

A. Airfoil in Rectilinear Motion

The noise model assumes a vertical gust w_g with the convection velocity U_c parallel to the x axis. This gust impinges on a flat plate airfoil situated between $-b < x < b$ and $-d < y < d$ in the x,y plane. The convection velocity U_c of the gust is eventually set equal to the free stream velocity U, but the initial derivation is performed with $U_c \neq U$. Imposing the condition of no flow through the airfoil surface leads to an unsteady surface dipole distribution leading to radiated noise. Linearized theory is assumed throughout.

The vertical gust is assumed to be produced by an incident turbulence field. The Karman spectrum is used as the basic model for the turbulence. This is modified later to include the effect of distortion produced by flow gradients.

1. Leading Edge Noise

A gust of the form

$$\tilde{\tilde{w}}_g = w_R(k_x, k_y)\, e^{-i[k_x(x - U_ct) + k_yy]} \tag{1}$$

is incident on the airfoil. In general this is a single Fourier component of a more complicated velocity field $w_g(x - U_ct, y)$ where

$$w_g(x - U_ct, y) = \int\int_{-\infty}^{\infty} \tilde{\tilde{w}}_g\, dk_x\, dk_y \tag{2}$$

The inverse Fourier relation is

$$w_R(k_x, k_y) = \frac{1}{(2\pi)^2} \int\int_{-R}^{R} w_g(x - U_ct, y)\, e^{i[k_x(x - U_ct) + k_yy]}\, dx\, dy \tag{3}$$

where R is a length scale indicating the region over which the gust velocity field extends. The convection velocity U_c can be a function of k_x and k_y.

When this gust impinges on the airfoil, a surface dipole distribution is induced to oppose the gust flow and satisfy the condition of no flow through the airfoil surface. This surface dipole distribution gives a pressure jump Δp across the airfoil; a normalized pressure jump g is defined as

$$\Delta p(x, y, t; k_x, k_y) = 2\pi\rho_0 U_c w_R(k_x, k_y)\, g(x, \bar{k}_x, \bar{k}_y, M)\, e^{i(k_x U_ct - k_yy)} \tag{4}$$

Integration over k_x and k_y then gives for the pressure jump due to all wavenumber components:

2

$$\Delta p(x,y,t) = 2\pi\rho_0 U_c \int\int\limits_{-\infty}^{\infty} W_R g \, e^{i(k_x U_c t - k_y y)} \, dk_x \, dk_y \qquad (5)$$

In the frequency domain

$$\Delta p_T(x,y,\omega) = 2\pi\rho_0 \int\limits_{-\infty}^{\infty} W_R(\lambda,k_y) \, g(x,\bar{\lambda},\bar{k}_y,M) \, e^{-ik_y y} \, dk_y \qquad (6)$$

where λ is the specific value of k_x such that $\lambda = \omega/U_c$ and the Fourier time integral is

$$F_T(\omega) = \frac{1}{2\pi} \int\limits_{-T}^{T} f(t) \, e^{-i\omega t} \, dt \qquad\qquad T \to \infty \qquad (7)$$

where $T = R/U_c$.

Knowing the force distribution produced by the fluid on the airfoil, the far-field noise can be calculated by noting that a force imposed on the fluid produces a dipole pressure field response. The far-field pressure of a point dipole situated at x_1, y_1, aligned with the z axis and with strength F_z exp($i\omega t$) is

$$p_0 = \frac{iF_z \omega z}{4\pi c_0 \sigma^2} \, e^{i[\omega t + \mu(Mx - \sigma)]} \, e^{-i\mu[Mx_1 - (xx_1 + \beta^2 yy_1)/\sigma]} \qquad (8)$$

where the observer is located at x,y,z and

$$\beta^2 \equiv 1 - M^2 \qquad\qquad K_x \equiv \omega/U$$

$$\mu \equiv MK_x/\beta^2 \qquad\qquad \sigma^2 \equiv x^2 + \beta^2(y^2 + z^2) \qquad (9)$$

Equation (8) gives the far-field sound produced by a point force and equation (6) gives the force at a point on the airfoil produced by the gust in terms of the airfoil response function. Combining and integrating over the airfoil planform gives the total far-field pressure. Thus,

$$p(\underline{x},\omega) = \frac{i\omega z \rho_0}{2c_0 \sigma^2} \, e^{i[\omega t + \mu(Mx - \sigma)]} \int\limits_{-d}^{d}\int\limits_{-b}^{b} e^{-i\mu[Mx_1 - (xx_1 + \beta^2 yy_1)/\sigma]}$$

$$\int\limits_{-\infty}^{\infty} W_R(\lambda,k_y) \, g(x_1,\bar{\lambda},\bar{k}_y,M) \, e^{-ik_y y_1} \, dk_y \, dx_1 \, dy_1 \qquad (10)$$

3

An effective lift function $\mathcal{L}$ per unit span can be defined as

$$\mathcal{L}(\bar{\lambda},\bar{k}_y,M) \equiv \frac{1}{b}\int_{-b}^{b} g(x_1,\bar{\lambda},\bar{k}_y,M)\, e^{-i\mu x_1(M - x/\sigma)}\, dx_1 \qquad (11)$$

This function includes retarded time effects in the propagation of the sound from the airfoil to the observer. For an observer overhead of the retarded source position ($x/\sigma = M$) equation (11) reduces to the lift/span.

It is assumed here that there is no spanwise variation of the airfoil characteristics (or at least little variation on the scale of the turbulence or other upwash disturbance). The y_1 integration in equation (10) can then be performed. For an airfoil situated between $-d < y < d$ (where d = semispan) the y_1 integration gives the factor

$$\Lambda \equiv \frac{2\sin[d(k_y - \mu\beta^2 y/\sigma)]}{k_y - \mu\beta^2 y/\sigma} \qquad (12)$$

so that from equation (10)

$$p_T(\underline{x},\omega) = i\,\frac{b\omega z\rho_0}{c_0\sigma^2}\, e^{i[\omega t + \mu(Mx - \sigma)]}\int_{-\infty}^{\infty} w_R(\lambda,k_y)\,\mathcal{L}(\bar{\lambda},\bar{k}_y,M)\,\Lambda\, dk_y \qquad (13)$$

In general, this final k_y integral cannot be evaluated in closed form. Thus, the integral must be evaluated numerically if an exact result is desired. However, for an airfoil span large compared to the dimensions of the upwash disturbance a simple approximation can be made. In this case ($\lambda d \gg 1$) the expression in equation (12) varies rapidly between positive and negative values, giving a cancelling effect, except where

$$k_y = \mu\beta^2 y/\sigma \equiv K_y \qquad (14)$$

Thus, the function in equation (12) acts like a delta function and w_0 and $\mathcal{L}$ can be moved outside the integral by setting $k_y = K_y$ in these functions. The remaining integral of $x^{-1}\sin x$ is equal to π; thus

$$p_T(\underline{x},\omega) = i\,\frac{\pi\omega b z\rho_0}{c_0\sigma^2}\, w_R(\lambda,K_y)\,\mathcal{L}(\bar{\lambda},\bar{K}_y,M)\, e^{i\mu(Mx - \sigma)} \qquad (15)$$

where the factor $\exp(i\omega t)$ has been omitted. This can be Fourier transformed using the inverse of equation (7) to find the far-field time history of the pressure; i.e.,

$$p(t) = \int_{-\infty}^{\infty} p_T(\omega)\, e^{i\omega t}\, d\omega \qquad (16)$$

Equations (15) and (16) give far-field expressions appropriate for the case of a deterministic velocity field such as the case of an airfoil cutting a vortex. The case of interest here is that of an

4

airfoil in a turbulent flow field for which the upwash velocity is not deterministic. The result for this case was derived in reference 1, and can be obtained from equation (15). Because infinite span airfoil response functions are used (thereby neglecting end effects) the problem is modeled as a turbulence region located between $-d < y < d$ incident on an infinite span airfoil. Also, the turbulence is assumed to be located between $-R < x < R$, where R is a large length scale that can later be allowed to approach infinity. This avoids convergence difficulties in the integrals that would appear if R were immediately set equal to infinity.

For a random function $f(y)$ which is nonzero between $-d < y < d$, the spectrum function ϕ is related to the Fourier transform of f by (see Appendix A)

$$\phi(k_y) = (\pi/d)\, E[F_d(k_y)\, F_d^*(k_y)] \tag{17a}$$

where E represents the expected value and

$$F_d(k_y) = \frac{1}{2\pi} \int_{-d}^{d} f(y)\, e^{-ik_y y}\, dy \tag{17b}$$

Equation (15) is multiplied by its complex conjugate and the expected value taken. Then using equation (17) the following relations hold

$$E[p_T(\omega)\, p_T^*(\omega)] = (T/\pi)\, S_{pp}(\omega)$$

$$E[w_R(\lambda,K_y)\, w_R^*(\lambda,K_y)] = (R\, d/\pi^2)\, \Phi_{ww}(\lambda,K_y) \tag{18}$$

Thus,

$$S_{pp}(\omega) = [\omega b z \rho_0/(c_0\sigma^2)]^2\, \pi U_c\, d\, |\mathcal{L}(\bar{\lambda},\bar{K}_y,M)|^2\, \Phi_{ww}(\lambda,K_y) \tag{19}$$

This agrees with equation (18) of reference 1.

2. Airfoil Response Functions

As discussed in reference 4, when calculating an approximate airfoil response function it is natural to divide the frequency range into a low and a high frequency regime. The ratio of airfoil chord to acoustic wavelength determines which regime is appropriate for a particular case.

For simplicity the case $U_c = U$ is considered; i.e., the incident disturbance convects at the free stream velocity. Thus, $\lambda = K_x$. The additional complexity is not needed here, but if results for the case $U_c \neq U$ are needed, they can be derived using the method of references 5 and 6.

For low frequency and an airfoil situated between $-1 < \bar{x} < 1$, the normalized pressure jump is found to be[5]

$$g(x,\bar{K}_x,0,M) = \frac{1}{\pi\beta}\sqrt{\frac{1-\bar{x}}{1+\bar{x}}}\ S(\bar{K}_x^*)\ e^{i\bar{K}_x^*[M^2\bar{x} + f(M)]} \qquad \bar{\mu} < 0.4 \tag{20}$$

5

where
$$f(M) \equiv (1 - \beta) \ln M + \beta \ln(1 + \beta) - \ln 2 \qquad K_x{}^* \equiv K_x/\beta^2$$

Here $S(\bar{k})$ is the Sears function[7] and the overbar on a quantity signifies normalization by the semichord b.

In deriving the airfoil response function for high frequency an iteration procedure is used which alternately corrects the boundary condition at the leading and trailing edges. The first two terms in this series are

$$g_1(x, \bar{K}_x, 0, M) = \frac{1}{\pi \sqrt{\pi(1 + M)\bar{K}_x(1 + \bar{x})}} \; e^{-i\Theta_3} \tag{21}$$

$$g_2(x, \bar{K}_x, 0, M) = \frac{1}{\pi \sqrt{2\pi(1 + M)\bar{K}_x}} [(1 + i)E^*(2\bar{\mu}(1 - \bar{x})) - 1] \; e^{-i\Theta_3}$$

with
$$\Theta_3 \equiv \bar{\mu}(1 - M)(1 + \bar{x}) + \pi/4 - \bar{K}_x$$

and where E^* is a combination of Fresnel integrals; i.e.,

$$E^*(x) \equiv \frac{1}{\sqrt{2\pi}} \int_0^x e^{-i\xi} \frac{d\xi}{\sqrt{\xi}} \tag{22}$$

By comparison with numerical results of Graham[8] these results for g are found to be accurate to within a few percent if the changeover from low to high frequency is made at the value $\bar{\mu} = 0.4$; the combination of the two functions becomes more accurate as $\bar{\mu}$ moves away from 0.4.

These values are for parallel gusts; i.e., $k_y = 0$. Values for $k_y \neq 0$ can readily be found for the case $U_c = U$ using the similarity results of Graham[8]. Depending on whether the gust-airfoil intersection point moves subsonically or supersonically relative to the fluid, the airfoil response function is similar to either the 3-D incompressible solution or the 2-D compressible solution respectively. Results are given here for the supersonic sweep speed case, but the results for the subsonic case readily follow if the appropriate analytical continuations of the various functions are employed.

For a gust-airfoil intersection that moves supersonically relative to the fluid, the airfoil response function is related to that for $k_y = 0$ by

$$g(x, \bar{K}_x, \bar{K}_y, M) = (\beta_\infty/\beta) g(x, \bar{K}_{x\infty}, 0, M_\infty) e^{ixK_y{}^2/K_x} \tag{23}$$

where
$$\beta_\infty{}^2 = \beta^2(1 + K_y{}^2/K_x{}^2) \qquad M_\infty{}^2 = M^2 - \beta^2 K_y{}^2/K_x{}^2$$

$$K_{x\infty}/\beta_\infty{}^2 = K_x/\beta^2 \qquad \mu_\infty = M_\infty K_{x\infty}/\beta_\infty{}^2 \tag{24}$$

6

This relation leads to the following results for g

$$g(x, \bar{K}_x, \bar{K}_y, M) = \frac{1}{\pi \beta} \sqrt{\frac{1 - \bar{x}}{1 + \bar{x}}} \; S(\bar{K}_x{}^*) \, e^{\, i[\mu M x + f(M_\infty) \bar{K}_x{}^*]} \qquad \bar{\mu}_\infty < 0.4 \qquad (25)$$

$$g_1(x, \bar{K}_x, \bar{K}_y, M) = \frac{1}{\pi \sqrt{\pi \bar{K}_x (1 + M_\infty)(1 + \bar{x})}} \; e^{-i\Theta_4} \qquad \bar{\mu}_\infty > 0.4 \qquad (26a)$$

$$g_2(x, \bar{K}_x, \bar{K}_y, M) = g_1(x, \bar{K}_x, \bar{K}_y, M) \; \sqrt{(1 + \bar{x})/2} \, [(1 + i) \, E^*(2\bar{K}_x{}^* M_\infty (1 - \bar{x})) - 1] \qquad (26b)$$

where

$$\Theta_4 \equiv \bar{K}_x{}^* [M_\infty (1 + \bar{x}) - M^2 \bar{x} - 1] + \pi/4$$

The effective lift $\mathcal{L}$ can be calculated using equation (4) to be

$$\mathcal{L}(\bar{K}_x, \bar{K}_y, M) = \beta^{-1} S(\bar{K}_x{}^*) \, e^{\, i \bar{K}_x{}^* f(M_\infty)} \, [J_0(\bar{\mu} x/\sigma) - i J_1(\bar{\mu} x/\sigma)] \qquad \bar{\mu}_\infty < 0.4 \qquad (27)$$

$$\mathcal{L}_1(\bar{K}_x, \bar{K}_y, M) = \frac{\sqrt{2}}{\pi \sqrt{\bar{K}_x (1 + M_\infty) \, \Theta_1}} \; E^*(2\Theta_1) \, e^{\, i\Theta_2} \qquad \bar{\mu}_\infty > 0.4 \qquad (28a)$$

$$\mathcal{L}_2(\bar{K}_x, \bar{K}_y, M) = \frac{e^{\, i\Theta_2}}{\pi \Theta_1 \sqrt{2\pi \bar{K}_x (1 + M_\infty)}} \left[i(1 - e^{-i2\Theta_1}) + (1 - i)[E^*(4\bar{K}_x M_\infty) \right.$$

$$\left. - \frac{\sqrt{2} \, e^{-i2\Theta_1}}{\sqrt{1 + (M/M_\infty)(x/\sigma)}} \; E^*(2\bar{\mu}(M_\infty/M + x/\sigma))] \right] \qquad (28b)$$

where

$$\Theta_1 \equiv \bar{\mu}(M_\infty/M - x/\sigma)$$

$$\Theta_2 \equiv \bar{\lambda} + \bar{\mu}(M - x/\sigma) - \pi/4 \qquad (29)$$

Here $\lambda = K_x$ so that Θ_2 reduces to $\Theta_2 = \bar{K}_x{}^*(1 - Mx/\sigma) - \pi/4$.

3. Spectrum Function – Karman spectrum

When the forcing function is a random phenomenon such as flow turbulence certain analytic expressions are available to represent the spectrum. A widely used model for isotropic turbulence is that of von Karman. For this model the spectrum is written

$$\Phi_{ww}(k_x, k_y, k_z) = \frac{E(k)}{4\pi k^2} \, (1 - k_z^2/k^2) \qquad (30)$$

for the three-wavenumber spectrum and

$$\Phi_{ww}(k_x, k_y) = \frac{4}{9\pi} \frac{\overline{u^2}}{k_e^2} \frac{\hat{k}_x^2 + \hat{k}_y^2}{1 + \hat{k}_x^2 + \hat{k}_y^2} \qquad (31)$$

7

for the two-wavenumber spectrum where

$$E(k) = \frac{Ik^4}{[1 + (k/k_e)^2]^{17/6}}$$

$$I = \frac{55}{9\sqrt{\pi}} \frac{\Gamma(5/6)}{\Gamma(1/3)} \frac{\overline{u^2}}{k_e^5} \tag{32}$$

$$k_e = \frac{\sqrt{\pi}}{L} \frac{\Gamma(5/6)}{\Gamma(1/3)}$$

and the circumflex on $\hat{k}$ signifies normalization by k_e. Further discussion of this spectrum function can be found in texts such as that of Hinze[9]. Also, additional results pertaining to the Karman spectrum are given in Appendix 1 of reference 1.

B. Airfoil in Circular Motion

With certain restrictions, the principles of the previous analysis for an airfoil in rectilinear motion can be applied to the case of a rotor. A flat plate airfoil of zero thickness can be represented by dipoles for both the case of rectilinear motion and circular motion (such as for a propeller). The far-field pressure for a dipole moving along a curved path was shown by Lowson[10] to be

$$p = \left[\frac{1}{4\pi c_0 r^2 (1 - M_n)^2} \; \underline{x} \cdot \left(\underline{f} + \frac{f \dot{M}_n}{1 - M_n} \right) \right] \tag{33}$$

where the square brackets imply evaluation at the retarded time and $\dot{M}_n \equiv \underline{M}_r \cdot \hat{n}$ is the acceleration component of the dipole in the direction of the observer. The $\underline{f}$ term represents the sound produced by an unsteady force and would be the same for the same force in rectilinear motion. The $\dot{M}_n$ term gives the sound produced by a force of constant strength under acceleration. If the frequency ω of the force is much greater than the rotational frequency Ω of the rotor, the $\underline{f}$ term is much greater than the $\dot{M}_n$ term, and it is as if the dipole were moving in rectilinear motion at that instant of time.

For incident turbulence noise of not too low a frequency, as well as being able to neglect the the $\dot{M}_n$ term, the blade force amplitude for a rotor is the same as for an airfoil moving in rectilinear motion. The high frequencies are produced by small eddies, and small eddies are cut completely by the airfoil before the airfoil undergoes any appreciable rotation, and this small rotation has an insignificant effect on the airfoil-eddy interaction.

Thus, the results of the previous section can be used to calculate the noise of a propeller or helicopter rotor at any instant of time. This result can be averaged over the period of rotation to obtain an average spectrum. This is a standard technique for time varying spectra as discussed by Bendat and Piersol[21]; it gives a result appropriate for comparison with measurements made by a spectral analyzer if the measurement time is significantly greater than the blade passage time.

The geometry of the problem is shown in Figure 1. The origin of the x,y,z coordinate system is fixed to the rotor hub with z along the rotor axis. The axial component of flow is in the negative z direction. The observer, fixed relative to the hub, is in the x,z plane at a distance r from the hub. The line from hub to observer makes an angle θ with the z axis. The vector $\underline{M}_f$, representing the non-axial component of flow, is at an angle ψ to the y axis; for $\psi = 180°$, $\underline{M}_f$ is along the y axis. The angle γ represents the angle the blade span makes with the x axis; i.e., $\gamma = \omega t$, and for $\gamma = 0$ the blade span lies along the x axis.

Because the blade is assumed to be a flat plate with zero steady loading, a blade segment makes an angle α with the x,y or azimuthal plane where

$$\cot \alpha = [M_t + M_f \cos(\gamma + \psi)]/M_z \tag{34}$$

and M_t is the azimuthal Mach number of the blade segment relative to the rotor hub. Due to the assumption of linearized theory, the blade segment need not be exactly aligned with the flow, but can be lightly loaded. The angle should not differ significantly from the value given by equation (34), however.

Because of the skewed inflow, there is a spanwise component $\underline{M}_a$ of flow over the blade where

$$\underline{M}_a = -M_f \sin(\gamma + \psi) \, (\hat{i} \cos \gamma + \hat{j} \sin \gamma) \tag{35}$$

9

The chordwise component $\underline{M}_b$ of the rotor segment Mach number is

$$\underline{M}_b = [M_t + M_f \cos(\gamma + \psi)] \, (-\hat{i} \sin \gamma + \hat{j} \cos \gamma) + \hat{k} \, M_z \qquad (36)$$

The expression given by equation (19) for the far-field of an airfoil in rectilinear motion is written in terms of the present airfoil position. In order to be able to apply this relation to the rotating airfoil segment, the equivalent of the present position must be calculated for the airfoil segment. This "present position" is the position of the airfoil segment relative to the fluid if it were to move along a rectilinear path during the time for the sound to propagate from the source to the observer. An alternative method is to rewrite equation (19) in terms of the retarded source position. Both methods should be of equal difficulty and should give the same results. The former is used here to remain consistent with previous publications by the author.

Both methods begin with a calculation of the retarded source position of the airfoil segment (or the rotor hub since distances on the order of the source size are not important when calculating the source position for a far-field observer). If at a time $t = 0$ a marker is placed in the fluid and a burst of sound is emitted, at time $t = T_e$, when the observer hears the sound burst, the marker has moved to position $\underline{x}_s$. The observer is at

$$\underline{x}_0 = r(\hat{i} \sin \theta + \hat{k} \cos \theta) \qquad (37)$$

The distance r_e of the observer from the retarded source point $\underline{x}_s$ is

$$r_e{}^2 = (r \sin \theta - x_s)^2 + y_s{}^2 + (r \cos \theta - z_s)^2 \qquad (38)$$

Also,

$$T_e = r_e / c_0 \qquad (39)$$

Since $\underline{M}_z$ and $\underline{M}_f$ are given by

$$\underline{M}_z = -M_z \, \hat{k}$$

$$\underline{M}_f = -M_f \, (\hat{i} \sin \psi + \hat{j} \cos \psi) \qquad (40)$$

the retarded source coordinates are

$$x_s = -T_e \, c_0 \, M_f \sin \psi = -M_f \, r_e \sin \psi$$

$$y_s = -M_f \, r_e \cos \psi \qquad (41)$$

$$z_s = - M_z \, r_e$$

Substitution of equation (41) into equation (38) leads to the following results for r_e

$$r_e = r \left[M_s \cos \Theta + \sqrt{1 - M_s{}^2 \sin^2 \Theta} \, \right] / (1 - M_s{}^2) \qquad (42)$$

where

10

$$\underline{M}_s \equiv \underline{M}_f + \underline{M}_z \qquad\qquad M_s^2 = M_f^2 + M_z^2$$

$$\tag{43}$$

$$M_s \cos \Theta = M_f \sin \psi \sin \theta + M_z \cos \theta$$

By calculating $(\underline{M}_s/M_s) \cdot (-\underline{x}_0)$, Θ is shown to be the angle between the convection Mach number $\underline{M}_s$ and the vector linking the observer and the source, $-\underline{x}_0$. Substitution of equation (42) into equation (41) determines the retarded source position $\underline{x}_s$.

The "present" source position $\underline{x}_p$ is found by adding to the retarded source vector a vector giving the chordwise airfoil movement during the time T_e. The spanwise component of fluid velocity is ignored here since it was ignored in deriving equation (19). This is allowable since in calculating the noise of an infinite span airfoil in rectilinear motion, any spanwise flow velocity can be eliminated by a coordinate transformation. The only purpose of calculating the "present" source position is to find the appropriate coordinates for use in equation (19). This position is

$$\underline{x}_p = \underline{x}_s + \underline{M}_b \, c_0 \, T_e \tag{44}$$

Introducing equations (41) and (36) into equation (44) gives

$$\underline{x}_p/r_e = -\hat{\imath}[M_t \sin \gamma + M_f \cos \gamma \sin (\gamma + \psi)] + \hat{\jmath}[M_t \cos \gamma - M_f \sin \gamma \sin (\gamma + \psi)] \tag{45}$$

For a coordinate system at this "present" source position the observer has coordinates $\underline{x}_1$ given by

$$\underline{x}_1 = \underline{x}_0 - \underline{x}_p \tag{46}$$

Equation (19) is appropriate for a coordinate system in which the flat plate airfoil lies in the x,y plane with the span along y. The $\underline{x}_1$ coordinate system above must be rotated to the same orientation with respect to the airfoil. Rotation of the $\underline{x}_1$ system about the z axis by an angle $\pi - \gamma$ gives a system which will be called the $\underline{x}_2$ system with y_2 pointed along the airfoil span. Rotation of the $\underline{x}_2$ system about the y_2 axis by an angle α gives the $\underline{x}_3$ system with x_3 along the chord pointing from leading to trailing edge. The relations between the $\underline{x}_1$ and $\underline{x}_3$ systems are

$$x_3 = (x_1 \sin \gamma - y_1 \cos \gamma) \cos \alpha - z_1 \sin \alpha$$

$$y_3 = x_1 \cos \gamma + y_1 \sin \gamma \tag{47}$$

$$z_3 = (x_1 \sin \gamma - y_1 \cos \gamma) \sin \alpha + z_1 \cos \alpha$$

The observer coordinates in the $\underline{x}_3$ system are the coordinates needed in equation (19). From equations (45) - (47) and equation (37) the observer coordinates in the $\underline{x}_3$ system are

$$x_3 = r_e M_t \cos \alpha - r_0 \cos \Phi$$

$$y_3 = x_0 \cos \gamma + M_f r_e \sin (\gamma + \psi) \tag{48}$$

$$z_3 = (x_0 \sin \gamma + r_e M_t) \sin \alpha + z_0 \cos \alpha$$

where

$$\cos \Phi = \cos \theta \sin \alpha - \sin \theta \sin \gamma \cos \alpha \qquad\qquad r_0^2 = x_0^2 + y_0^2 + z_0^2 \tag{49}$$

11

Φ is the angle between the x_3 axis and the line from the observer to the rotor blade segment. This can be seen by replacing $\underline{x}_1$ by $\underline{x}_0$ in the expression for x_3 given by equation (49) and substituting for $\underline{x}_0$ using equation (37).

1. With No Blade-Blade Correlation

Equations (48) – (49) give the appropriate "instantaneous observer coordinates" to use in calculating the sound spectrum from equation (19). The angle $\gamma = \omega t$ is a function of time. In order to calculate the time averaged spectrum, an average around the azimuth must be determined. This average must account for both the Doppler shifting of frequency as the airfoil segment moves relative to the observer, and the retarded time effects as the blade moves around the azimuth. The latter correction is needed because the blade spends different amounts of time, in the acoustic sense, at each azimuthal location. As noted in reference 12, the proper azimuthal weighting is the factor ω/ω_0 where ω is the frequency of the airfoil forces and ω_0 is the Doppler shifted frequency. The azimuthally averaged spectrum is then

$$S_{pp}(\underline{x},\omega) = \frac{1}{2\pi} \int_0^{2\pi} \frac{\omega}{\omega_0} \, S'_{pp}(\underline{x},\omega_0,\gamma) \, d\gamma \tag{50}$$

The spectrum $S'_{pp}(\underline{x},\omega_0,\gamma)$ for the case of relative motion between source and observer is related to $S_{pp}(\underline{x},\omega,\gamma)$ with no relative motion by the Doppler factor ω/ω_0; i.e., as shown in reference 13,

$$S'_{pp}(\underline{x},\omega_0,\gamma) = (\omega/\omega_0) \, S_{pp}(\underline{x},\omega,\gamma) \tag{51}$$

Thus, equation (50) and (51) together introduce a factor $(\omega/\omega_0)^2$.

The Doppler factor ω/ω_0 is shown in references 12 and 13 to be

$$\frac{\omega_0}{\omega} = 1 + \frac{\underline{M}_t \cdot \hat{SO}}{1 - \underline{M}_r \cdot \hat{SO}} \tag{52}$$

where
$\underline{M}_t$ = Mach number of source relative to observer
$\underline{M}_r$ = Mach number of source relative to fluid
$\hat{SO}$ = unit vector from retarded source position to observer.

In vector notation

$$\underline{M}_t = M_t \, (-\hat{i} \sin \gamma + \hat{j} \cos \gamma)$$

$$\underline{M}_r = \hat{i} \, (M_f \sin \psi - M_t \sin \gamma) + \hat{j} \, (M_f \cos \psi + M_t \cos \gamma) + \hat{k} \, M_z \tag{53}$$

$$\underline{OS} = \hat{i} \, (x - x_s) + \hat{j} \, (y - y_s) + \hat{k} \, (z - z_s)$$

Using equation (41) and the fact that $|\underline{OS}| = r_e$ gives the unit vector

12

$$S\hat{\ }O = \hat{i}\,(x/r_e + M_f \sin\psi) + \hat{j}\,M_f \cos\psi + \hat{k}\,(z/r_e + M_z) \tag{54}$$

and finally from equation (65) and $S\hat{\ }O = -O\hat{\ }S$

$$\frac{\omega}{\omega_0} = 1 + \frac{M_t[x \sin\gamma - M_f r_e \cos(\gamma + \psi)]}{(1 - M_s^2)r_e - x M_f \sin\psi - z M_z}$$

$$= 1 + \frac{M_t[x \sin\gamma - M_f r_e \cos(\gamma + \psi)]}{\sqrt{1 - (M_f^2 + M_z^2)\sin^2\Theta}} \tag{55}$$

The final result for the azimuthally averaged spectrum is given by equation (50), (51) and (55) with $S_{pp}(\underline{x},\omega,\gamma)$ in equation (51) given by equation (19). The x,y,z coordinates to be used in equation (19) are x_3, y_3, z_3, respectively, given by equation (48).

2. With Blade-Blade Correlation

The technique of averaging the instantaneous spectrum around the azimuth is valid if there is no correlation between the spectra for points widely separated in time. For the case of turbulence interaction, however, this is not necessarily true. The larger turbulent eddies can be cut more than once while passing through the rotor plane and the spectra from these events are correlated.

For the case where blade-blade correlation exists, the autocorrelation function would consist of a series of peaks, such as shown in Figure 2, the n'th peak representing the correlation of sound from the zeroth blade with that of the n'th blade. The correlation function for the multiple blade passage case can be written

$$R_{pp}(\underline{x},\gamma,\tau) = \sum_{n=-\infty}^{\infty} R_{pp}^{(n)}(\underline{x},\gamma,\tau - nT_2) \tag{56}$$

where $R_{pp}^{(n)}$ represents the cross-correlation of the far-field sound from the n'th blade with that from the zeroth blade. The time T_2 is the time, as heard by an observer, between blade chops of any given eddy.

Figure 3 illustrates the geometry of the multiple chopping. The blades move along line AD. The blades are assumed to be moving rectilinearly in the vicinity of the eddy; this is a reasonable assumption provided that the eddies are not too large. The eddy moves in the chordwise direction relative to the airfoil with Mach number $\underline{M_b}$ given by equation (36). After a time T_1 the eddy has moved down from the rotor plane a distance

$$FE = T_1 V_z \tag{57}$$

and in the plane a distance

$$FC = T_1 V_f \cos(\gamma + \psi) \tag{58}$$

At time T blade 1 is at point C; the distance BC is

$$BC = (T - T_1) V_t \tag{59}$$

The distance Z is then

$$Z^2 = BF^2 + FE^2 = T_1^2 V_z^2 + [(T - T_1) V_t - T_1 V_f \cos (\gamma + \psi)]^2 \tag{60}$$

This distance is the minimum between the lines ED and BG if BE is normal to these two lines. For this to be true, $BD^2 = BE^2 + ED^2$ or

$$Z^2 = T^2 V_t^2 - T_1^2 \{V_z^2 + [V_t + V_f \cos(\gamma + \psi)]^2\} \tag{61}$$

Equations (73) and (74) can be solved for T_1 and Z giving

$$T_1 = T (V_t/V_z) \sin \alpha \cos \alpha \qquad\qquad Z = T V_t \sin \alpha \tag{62}$$

Equation (19) for the far-field spectrum of an airfoil was obtained by multiplying equation (15) by its complex conjugate and taking the expected value. The equation for the n'th blade passage is equation (15) with the additional factor $\exp(ik_z nZ)$ to account for the z_3 distance nZ of the n'th blade path from the zeroth blade path as measured with respect to the fluid.

The time T_2 is the time T_1 plus the additional time difference for the sound from point B in Figure 3 to reach the observer as compared to the time for the sound from point C to reach the observer. From the last factor in equation (15), the time for the sound to reach the observer from point C is

$$\tau_0 = (M_b x - \sigma)/(c_0 \beta_b^2) \tag{63}$$

Replacing x by x + X and y by y − Y where

$$X \equiv BC = (T - T_1) V_t \qquad\qquad Y = T_1 V_f \sin (\gamma + \psi) \tag{64}$$

gives the time T_1 for the sound to propagate from point B. Taking the difference between T_1 and τ_0,

$$\Delta\tau = X (M_b - x/\sigma)/(\beta_b^2 c_0) + Y y/(c_0 \sigma) = T_2 - T_1 \tag{65}$$

Then, T_2 can be determined from equations (62), (64) and (65).

Taking the Fourier transform of equation (56) gives

$$S'_{pp}(\underline{x}, \omega_0, \gamma) = \sum_{n = -\infty}^{\infty} S'^{(n)}_{pp}(\underline{x}, \omega_0, \gamma) e^{in\omega_0 T_2} \tag{66}$$

The cross PSD, $S_{pp}^{(n)}$ is found by multiplying equation (15) by its complex conjugate with the additional factors $\exp(ik_z Zn)$ as noted before, or from equations (19) and (51)

$$S'^{(n)}_{pp}(\underline{x},\omega_0,\gamma) = \int_{-\infty}^{\infty} \left(\frac{\omega z \rho_0 b}{c_0 \sigma^2}\right)^2 \pi U_b d(\omega/\omega_0) |\mathcal{L}(\lambda,K_y,M)|^2 \, \Phi_{ww}(\lambda,K_y,k_z) e^{ik_z nZ} \, dk_z \tag{67}$$

Introducing equation (67) into equation (66) and using the identity

14

$$\sum_{n=-\infty}^{\infty} e^{i2\pi na} = \sum_{n=-\infty}^{\infty} \delta(n+a) \tag{68}$$

gives

$$S'_{pp}(\underline{x},\omega_0,\gamma) = \left(\frac{\omega z \rho_0 b}{c_0 \sigma^2}\right)^2 \pi U_b d\ (\omega/\omega_0)\ |\,\mathcal{L}(\lambda,K_y,M)|^2\ \overline{u^2}\ b^2 \sum_{n=-\infty}^{\infty} \Phi_{ww}(\lambda,K_y,K_z^{(n)})\ \frac{2\pi}{b^2\ \overline{u^2}\ Z} \tag{69}$$

where

$$K_z^{(n)} = (\omega_0 T_2 + 2\pi n)/Z \tag{70}$$

15

C. Turbulence Contraction

The analysis used here for calculating the spectrum of turbulence being subjected to a rapid contraction follows the general method of Ribner and Tucker[15]. It has been generalized slightly to allow for non diagonal deformation tensors, although in principle these results could be derived from the Ribner and Tucker results by first transforming to principle coordinates. The analysis is based on the fact that vorticity follows the flow. There is assumed to be no interaction of the vorticity with itself. The details of the analysis are presented in reference 17. A summary of the necessary equations is given below, and a fuller derivation is given in Appendix B.

The upstream and downstream coordinate systems are designated by the two coordinate systems e^u and e^d respectively where e is a matrix $e(i,j)$ composed of the three unit vectors along the axes. $e(i,1)$, $e(i,2)$ and $e(i,3)$ denote the three components of the unit vectors parallel to the local vorticity vector $\underline{\Omega}$, the local turbulence velocity and the unit vector in the direction of the wavevector, respectively. The relation between $e(i,1)^u$ and $e(j,1)^d$ is readily obtained from the knowledge that vortex lines follow fluid particles. The relation is then obtained from the Cauchy relation

$$\Omega_i{}^u = \Omega_j{}^d (\partial x_i / \partial \xi_j) \tag{71}$$

where $\partial x_i / \partial \xi_j$ represents the deformation tensor, x_i represents the upstream particle coordinates and ξ_j represents the downstream particle coordinates. In the computer programs $\partial x_i / \partial \xi_j$ is represented by DXDZ(I,J). The relation between $e^u(i,3)$ and $e^d(i,3)$ can be found by consideration of the manner of distortion of a sheet of vorticity between upstream and downstream: since vorticity follows the fluid, a pair of vectors lying in this plane upstream also lie in the corresponding downstream plane, and the wavevector is normal to the plane. First assume that $e^d(i,j)$ is given. Thus, if $\Omega_j{}^d$ is replaced in turn by $e^d(i,1)$ and $e^d(i,2)$, two vectors are found, the cross product of which lies along $e^u(i,3)$. The remaining vector $e^u(i,2)$ can then be found by the cross product of $e^u(i,1)$ and $e^u(i,3)$.

Knowing the relation between $e^u(i,j)$ and $e^d(i,j)$, the relation between the downstream and upstream wavenumbers is given in Reference 17 as

$$k^d / k^u = e^u(i,3) \, e^d(j,3) \, \partial x_i / \partial \xi_j \tag{72}$$

The relation between fluid velocities is

$$q_i{}^u(\underline{k}^u) = q^d(\underline{k}^d) f_1{}^u e(i,2) \, k^d / k^u \tag{73}$$

where $f_1{}^u$ is the magnitude of the vector found by replacing $\Omega_j{}^d$ in equation (71) by $e(j,1)$.

16

References

1. Amiet, R. K.: "Acoustic Radiation from an Airfoil in a Turbulent Stream". *J. Sound and Vibration*, Vol. 41, 1975, pp. 407-420.

2. Paterson, R. W. and Amiet, R. K.: "Noise and Surface Pressure Response of an Airfoil to Incident Turbulence". *J. Aircraft*, Vol. 14, 1977, pp. 729-736.

3. Amiet, R. K.: "Noise Due to Rotor-Turbulence Interaction". NASA Conference Publication 2052, 1978, pp 109-126.

4. Amiet, R. K.: "Effects of Compressibility in Unsteady Airfoil Lift Theories". Published in <u>Unsteady Aerodynamics</u>, Proceedings of a Symposium on Unsteady Aerodynamics, University of Arizona, Tucson, March 18-20, 1975, pp. 631-653, Edited by R. B. Kinney.

5. Amiet, R. K.: "Compressibility Effects in Unsteady Thin-Airfoil Theory". *AIAA Journal*, Vol. 12, 1974, pp. 253-255.

6. Amiet, R. K.: "High Frequency Thin-Airfol Theory for Subsonic Flow". *AIAA Journal*, Vol. 14, 1976, pp. 1076-1082.

7. von Karman, T. and Sears, W. R.: "Airfoil Theory for Non-Uniform Motion". *J. Aeronautical Sciences*, Vol. 5, 1938, pp. 379-390.

8. Graham, J. M. R.: "Similarity Rules for Thin Aerofoils in Non-Stationary Subsonic Flows". *J. Fluid Mech.*, Vol. 43, 1970, pp. 753-766.

9. Hinze, J. O.: <u>Turbulence</u>, McGraw Hill, Inc., New York, 1975.

10. Lowson, M. V.: "The Sound Field for Singularities in Motion", Proc. Royal Society, Vol. A286, 1965, pp. 559-572.

11. Bendat, J. S. and Piersol, A. G.: <u>Measurement and Analysis of Random Data</u>. John Wiley and Sons, Inc., 1966, p. 365.

12. Amiet, R. K.: "Noise Produced by Turbulent Flow into a Propeller or Helicopter Rotor". AIAA Paper 76-560, 1976. Condensed version given in *AIAA Journal*, Vol. 15, 1977, pp. 307-308.

13. Amiet, R. K.: "Frame of Reference Considerations for the Forward Flight Noise Problem". UTRC Report N212775-1, 1974.

14. Amiet, R. K.: "The Spectrum of Turbulence Undergoing a Rapid Distortion". UTRC Report UTRC84-26, 1984

15. Ribner, H. S. and Tucker, M.: "Spectrum of Turbulence in a Contracting Stream." NACA Report 1113, 1952.

16. Lamb, H.: <u>Hydrodynamics</u>. Sixth edition, 1932, Dover Publications, New York, p. 205.

17. Simonich, J. C., Amiet, R. K., Schlinker, R. H. and Greitzer, E. M.: Helicopter Rotor Noise Due to Ingestion of Atmospheric Turbulence, NASA CR3973, 1986.

List of Symbols

B	Blade number
b	Airfoil semichord
c	Airfoil chord
c_0	Sound speed
d	Airfoil semispan
$E[.]$	Expected value operator
$E(k)$	Energy spectrum; see Eq. (32)
E^*	Fresnel integrals; see Eq. (22)
f_0	Frequency measured by observer
$f(M)$	Function of Mach number; see Eq. (20)
g	Normalized airfoil response function; see Eq. (4)
I	Factor defined by Eq. (32)
$\hat{i}, \hat{j}, \hat{k}$	Unit vectors in the x, y and z directions
J_0, J_1	Bessel functions
k_x, k_y	x and y wavenumbers
k_e	Wavenumber defined by Eq. (32)
K_x	ω/U
K_x^*	K_x/β^2
K_y	$\mu\beta^2 y/\sigma$
L	Turbulence integral length scale
$\mathcal{L}$	Effective lift; see Eq. (11)
M	Free stream Mach number
$\underline{M}_a$	Spanwise flow Mach number over blade
$\underline{M}_b$	Chordwise Mach number of blade
$\underline{M}_f$	Flight Mach number in rotor plane
$\underline{M}_r$	Mach number of rotor segment relative to fluid
$\underline{M}_t$	Mach number of blade segment relative to rotor hub
$\underline{M}_z$	Flow Mach number along rotor axis
$\hat{O^S}$	Unit vector from retarded source to observer
p_T	Fourier time transform of p
Δp	Pressure jump on airfoil produced by all gusts
p_0	Far-field pressure of dipole
$\underline{Q}$	Magnitude of turbulent velocity in Appendix B
$\underline{q}$	Turbulent velocity in Appendix B
r_e	Distance from observer to retarded source
r_0	Distance of observer from rotor hub
r	$-x$
R	Integration limit for spatial Fourier transform
R_{pp}	Autocorrelation of far-field sound
$R_{pp}^{(n)}$	Cross correlation of far-field sound from n'th blade with that of zeroth blade
R_{qq}	Cross spectrum of airfoil surface pressure
S_{pp}	Far-field acoustic spectrum for observer fixed relative to blade segment
S'_{pp}	Far-field acoustic spectrum for observer fixed relative to blade hub
T	Time between blade passes
T_1	Time between eddy chops

T_2	Time between eddy chops as heard by observer
T_e	Time between emission and reception of sound
t	Time
$\overline{u^2}$	Mean square turbulence level
U	Stream velocity
U_b	Component of fluid velocity along airfoil chord
U_c	Turbulence convection velocity
V_f	Flow velocity in rotor plane
V_t	Azimuthal velocity of airfoil segment
V_z	Axial flow velocity
w_g	Gust velocity
w_R	Spatial Fourier transform of gust velocity
x,y,z	Cartesian coordinate system; flow along x and y along span
$\underline{x}_0$	Vector from rotor hub to observer
$\underline{x}_s$	Vector from rotor hub to retarded source position
$\underline{x}_p$	Hypothetical "present source position" defined by Eq. (44)
$\underline{x}_1$	Vector from "present source position" to observer
$\underline{x}_3$	Observer position in rotated coordinate system
X	Distance defined by Eq. (64)
Y	Distance defined by Eq. (64)
Z	Distance defined by Eq. (62)
α	Out of plane angle of rotor blade
β^2	$1 - M^2$
$\beta_b{}^2$	$1 - M_b{}^2$
Γ	Gamma function
γ	Azimuthal blade angle
Θ	Angle defined by Eq. (43)
Θ_1, Θ_2	Functions defined by Eq. (29)
θ	Angle of observer from upstream rotor axis
λ	ω/U_c; also, in Appendix B this is the wavelength
μ	MK_x/β^2
ρ_0	Density of air
σ^2	$x^2 + \beta^2(y^2 + z^2)$
τ_0	Time between eddy chop and when observer hears it
Φ	Angle defined by Eq. (49)
Φ_{ww}	Velocity spectrum of turbulence
ψ	Angle of flow in rotor plane; see Fig. 1
ω	Radian frequency measured by observer fixed relative to rotor hub; also, vorticity in Appendix B.
ω_0	Doppler shifted radian frequency measured by observer fixed to rotor hub
$\tilde{\omega}$	$\omega\delta^*/U$
$\sim$	Fourier transformed variable
Overbar	Normalized by semichord b
Subscript	Denotes similarity variable; see Eq. (28)

19

Appendix A: Relation of Fourier Transform of a Random Function to Its Spectrum

If $f(y)$ is a random function of y between $-\infty < y < \infty$, the infinite Fourier transform between these limits is not defined, in general, because of convergence problems. If, however, finite limits are placed such that $f(y)$ is random between $-d < y < d$ and $f(y)$ is zero outside this range, a Fourier transform

$$F_d(k_y) = \frac{1}{2\pi} \int_{-d}^{d} e^{-ik_y y} \, f(y) \, dy \tag{A1}$$

can be defined for any particular sample $f(y)$. The cross correlation function R is

$$R(\eta) = E[f(y + \eta) \, f(y)] \tag{A2}$$

The spectrum ϕ is the Fourier transform of R so that

$$\phi(k_y) = \frac{1}{2\pi} \int_{-\infty}^{\infty} R(\eta) \, e^{-ik_y \eta} \, d\eta = \frac{1}{2\pi} \int_{-\infty}^{\infty} E[f(y + \eta) \, f(y)] \, e^{-ik_y \eta} \, d\eta$$

$$= \frac{1}{2\pi} E \left[f(y) \int_{-d}^{d} f(\zeta) \, e^{ik(y - \zeta)} \, d\zeta \right] \tag{A3}$$

$$= E \left[F_d(k_y) \, e^{ik_y y} \, f(y) \right]$$

Integration over y then gives

$$2d \, \phi(k_y) = 2\pi \, E [\, F_d(k_y) \, F_d^*(k_y) \,] \tag{A4}$$

which is equation (17).

Appendix B: The Spectrum of Turbulence Undergoing a Rapid Distortion

The following analysis calculates the change in wavevector and fluid velocity for a turbulent flow undergoing a rapid contraction. A sketch of the problem is shown in figure 4. The analysis begins in Section 1 by deriving the relations between vorticity and velocity for a particular wavevector component at a point. These results are derived from the assumed sinusoidal variation for the velocity field of a wavevector component.

In section 2 the equations for the transport of vorticity are used to derive a relation between the pre-contraction and post-contraction velocity vectors of a wavevector component. In section 3 the same transport equations are used to derive a relation between the pre-contraction and post-contraction wavevectors.

Finally, in section 4 the results are compared to the results of Ribner and Tucker. Agreement is found for both the wavevector and the fluid velocity transformation.

1. Relations Between Velocity and Vorticity

In calculating the noise generated by a rotor moving through a turbulent field, a required input is the turbulence spectrum as a function of the wavevector

$$\underline{k} = \hat{\imath}\, k_x + \hat{\jmath}\, k_y + \hat{k}\, k_z \tag{B1}$$

The velocity field $\underline{q}$ of a single wavevector Fourier component can be written

$$\underline{q}^d(\underline{k}^d, \underline{x}) = \underline{Q}^d(\underline{k}^d)\, e^{i\underline{k}^d \cdot \underline{x}} \tag{B2}$$

where the d superscript refers to the downstream or post-contraction location, at the rotor face. The superscript u will refer to the upstream pre-contraction velocity field. The object of this section is to relate the two velocity fields. In equation (B2) $\underline{Q}$ and $\underline{k}$ are orthogonal from the assumption of incompressible flow (see figure 5). Thus, $\underline{Q}$ can be written as the cross product of $\underline{k}$ with some vector $\underline{P}$; i.e.,

$$\underline{Q}(\underline{k}) = \underline{k} \times \underline{P}(\underline{k}) \tag{B3}$$

The superscripts u and d are not used here since the equation can be applied to either region.

The vorticity field $\underline{\omega}$ of the wavevector Fourier component is given by

$$\underline{\omega} = \nabla \times \underline{q} \tag{B4}$$

so that from equations (B2) and (B3)

$$\underline{\omega}(\underline{k},\underline{x}) = i\underline{k} \times \underline{Q}(\underline{k})\, e^{i\underline{k} \cdot \underline{x}} = i[\underline{k}(\underline{k} \cdot \underline{P}) - \underline{P}\, k^2]\, e^{i\underline{k} \cdot \underline{x}} \tag{B5}$$

From equation (B5) it will be noted that

21

$$\underline{k} \cdot \underline{\omega} = 0 \tag{B6}$$

Writing

$$\underline{\omega}(\underline{k},\underline{x}) = \underline{\Omega}(\underline{k})\, e^{i\underline{k}\cdot\underline{x}} \tag{B7}$$

$\underline{Q}$ is to be solved for in terms of $\underline{\Omega}$. Then, knowing how $\underline{\Omega}$ transforms between pre-contraction and post-contraction locations, the behavior of the velocity field will be known. From equations (B5) and (B7)

$$\underline{\Omega}(\underline{k}) = i\,[\underline{k}(\underline{k}\cdot\underline{P}) - \underline{P}k^2] \tag{B8}$$

On taking the cross product of this equation with $\underline{k}$, the first term on the right hand side drops out leaving

$$\underline{k} \times \underline{\Omega} = -ik^2\,\underline{k} \times \underline{P} = -ik^2\,\underline{Q} \tag{B9}$$

This gives two equivalent expressions for relating vorticity and velocity of a Fourier component

$$\underline{\Omega} = i\,\underline{k} \times \underline{Q} \qquad\qquad \underline{Q} = i\,\underline{k} \times \underline{\Omega}/k^2 \tag{B10}$$

2. Relating Pre-contraction and Post-contraction Velocities

The relations between pre-contraction and post-contraction are now considered. The vorticity of a fluid particle is related by the deformation tensor. Using an expression attributed to Cauchy[16]

$$\Omega_i{}^d = \Omega_j{}^u\,\partial\xi_i/\partial x_j \qquad\qquad \Omega_i{}^u = \Omega_j{}^d\,\partial x_i/\partial\xi_j \tag{B11}$$

where x_i represents the pre-contraction coordinate system and ξ_i the post-contraction coordinate system. Both coordinate systems are assumed right-handed and orthogonal. The coordinates of a fluid particle also transform according to equation (B11). For example, consider a cube of post-contraction fluid with edges parallel to the axes. The edges can then be written $(\ell,0,0)$, $(0,\ell,0)$, $(0,0,\ell)$ where ℓ is the length of the side of the cube. By writing each of these vectors as a row vector, the three together form a 3×3 matrix C^d which can be written

$$C^d = \ell\, I \tag{B12}$$

where I is the unity matrix. The three upstream transformed vectors denoting the cube are then given by

$$C^u = C^d\,[\partial x_i/\partial\xi_j] = \ell\,[\partial x_i/\partial\xi_j] \tag{B13}$$

where $[\partial x_i/\partial\xi_j]$ denotes the deformation tensor defined as

22

$$\partial x_i / \partial \xi_j = \begin{bmatrix} \partial x_1/\partial \xi_1 & \partial x_1/\partial \xi_2 & \partial x_1/\partial \xi_3 \\ \partial x_2/\partial \xi_1 & \partial x_2/\partial \xi_2 & \partial x_2/\partial \xi_3 \\ \partial x_3/\partial \xi_1 & \partial x_3/\partial \xi_2 & \partial x_3/\partial \xi_3 \end{bmatrix} \qquad (B14)$$

The pre-contraction volume of the cube is then given by the cross product of two of the vectors with the dot product of the third, which is the same as the value of the determinant of the matrix. For incompressible flow this must be ℓ^3, the same as the post-contraction value. This requires that the determinant of the deformation matrix in equation (B14) be 1.

The following paragraphs will give the detailed procedure for transforming between pre-contraction and post-contraction velocity fields. One basic assumption of the analysis to follow is that fluid planes in one coordinate system remain planes after deformation. This assumption will be grossly incorrect, in general, on a large scale. However, it becomes more and more accurate as restriction to smaller and smaller scales is made. The assumption should thus be adequate if the turbulence scale is small compared to the scale of the distorted flow. The assumption arises when a one-to-one correspondence is made between a pre-contraction and a post-contraction Fourier component of the turbulence. Each Fourier component consists of a vorticity distribution over all space, whereas the deformation tensor is a function of position, and the flow is distorted by different amounts at different points.

The relation between the pre-contraction and post-contraction wavevectors has yet to be determined. For the present they will be denoted by $\underline{k}^u$ and $\underline{k}^d$ with the assumption that the two wavevectors are related by the deformation tensor in some manner to be determined later. Equations (B10) and (B11) can then be combined to obtain a relation between the pre-contraction and post-contraction velocity field. Equations (B11) relate pre-contraction and post-contraction vorticity levels while equations (B10) relate velocity to vorticity at either pre-contraction and post-contraction location.

Combining equations (B10b) and (B11b) gives

$$Q_i^u(\underline{k}^u) = i \, (k_j^u/k^{2u}) \, \Omega_n^d(\underline{k}^d) \, (\partial x_k/\partial \xi_n) \, \epsilon_{ijk} \qquad (B15)$$

where Cartesian tensor notation is used. Summation over repeated indices is assumed, and ϵ_{ijk} is the alternating tensor. Using equation (B10a) to substitute for Ω_n^d gives

$$Q_i^u(\underline{k}^u) = - \, (k_j^u/k^{2u}) \, k_l^d Q_m^d(\underline{k}^d) \, \epsilon_{lmn} \, (\partial x_k/\partial \xi_n) \, \epsilon_{ijk} \qquad (B16)$$

This equation relates the pre-contraction and post-contraction velocities if the relation between the pre-contraction and post-contraction wavevectors $\underline{k}^u$ and $\underline{k}^d$ is known; this relation will be determined shortly. It should be noted that although the spatial coordinates of the pre-contraction and post-contraction locations do not appear explicitly, they do appear implicitly through the deformation tensor. Thus, even though the velocity field has been decomposed into spatial Fourier components, this is in some sense a local decomposition.

In applying equation (B16), in addition to specifying the deformation tensor and wavevector of interest, the velocity $\underline{Q}^d$ must be specified. The amplitude of $\underline{Q}^d$ is not of concern since the ratio of amplitudes is all that is needed. The direction of $\underline{Q}^d$ must be specified, however. Once $\underline{k}^d$ is specified,

$\underline{Q}^d$ can lie anywhere in the plane normal to $\underline{k}^d$ since $\underline{k}^d$ and $\underline{Q}^d$ are normal for the velocity modes considered. For the specific case of an airfoil moving through the turbulent field consider a plane formed by the vector $\underline{k}^d$ and a unit vector $\hat{n}$ normal to the airfoil surface. Then for the specific $\underline{k}^d$ vector chosen, the velocity field can be decomposed into a component in the plane formed by the vectors $\underline{k}^d$ and $\hat{n}$ and a component normal to this plane. In calculating the airfoil response to turbulence using a linearized analysis, only the velocity component along $\hat{n}$ will give a contribution. Thus, any component of $\underline{Q}^d$ normal to the $\underline{k}^d$, $\hat{n}$ plane can be neglected. This allows $\underline{Q}^d$ to be specified as normal to $\underline{k}^d$ and in the $\underline{k}^d$, $\hat{n}$ plane.

3. Relating Pre-contraction and Post-contraction Wavevectors

The only remaining relation to be determined in equation (B 16) is that between $\underline{k}^u$ and $\underline{k}^d$; i.e., how the wavevectors of the mode considered become distorted in going from upstream to downstream. As with $\underline{Q}^u$ and $\underline{Q}^d$, the wavevectors will be related through the deformation tensor. The three vectors $\underline{\Omega}^d$, $\underline{Q}^d$ and $\underline{k}^d$ form an orthogonal system. In addition, $\underline{k}^d$ is assumed to be in the direction $\underline{\Omega}^d \times \underline{Q}^d$ so that the system is right handed. Define vectors $\hat{e}_1^{d,u}$, $\hat{e}_2^{d,u}$, $\hat{e}_3^{d,u}$ along $\underline{\Omega}^{d,u}$, $\underline{Q}^{d,u}$, and $\underline{k}^{d,u}$ respectively where either d or u is read, not both. First the relations between $\hat{e}^u$ and $\hat{e}^d$ will be determined and then the relation between $\underline{k}^u$ and $\underline{k}^d$. As a matter of notation, note that subscripts here can refer to either components of a vector as in the Cartesian tensor notation of equation (B 16), or to a specific vector such as $\hat{e}_1$, $\hat{e}_2$, $\hat{e}_3$. Generally the meaning will be clear from the context since $\hat{e}$ already indicates a vector and the subscripts 1,2 or 3 then indicate a specific vector, not the component of a vector.

The relation between $\hat{e}_1^u$, $\hat{e}_1^d$ is readily obtained from the knowledge that vortex lines follow fluid particles. Since $\hat{e}_1$ is parallel to $\underline{\Omega}$, equation (B 11) immediately gives $\hat{e}_1^d$; i.e., if $\underline{f}_1$ defines the direction of $\hat{e}_1^u$, then

$$(f_1^u)_i = (e_1^d)_j \, (\partial x_i / \partial \xi_j) \qquad\qquad \hat{e}_1^u = \underline{f}_1^u / |\underline{f}_1^u| \qquad\qquad (B17)$$

where the j subscript on e^d now indicates one of the three Cartesian components of the vector $\hat{e}_1^d$. Also, the summation convention over repeated indices is assumed.

To calculate the vector $\hat{e}_2^u$, it is not sufficient to merely substitute subscripts 2 for 1 in equation (B 17). The resulting vector so defined would not necessarily be orthogonal to $\hat{e}_1^u$. Therefore a different approach will be used, first calculating $\hat{e}_3^u$, then $\hat{e}_2^u$. First define a vector

$$(f_2^u)_i = (e_2^d)_j \, (\partial x_i / \partial \xi_j) \qquad\qquad (B18)$$

As noted above, this vector will not in general be orthogonal to $\hat{e}_1^u$. However, it will lie in the same plane of vorticity as $\hat{e}_1^d$ and $\hat{e}_2^d$. For example, consider a plane of vortex lines defined by the vectors $\hat{e}_1^d$ and $\hat{e}_2^d$. Because the vorticity moves with the fluid and because equation (B 18) is a Lagrangian type of equation following fluid particles, $\underline{f}_2^u$ must lie in the same plane of vortex lines. Thus, although $\hat{e}_2^u$ hasn't yet been determined, $\hat{e}_3^u$ can be found since it must be normal to the plane defined by $\hat{e}_1^u$ and $\underline{f}_2^u$; i.e.,

$$\hat{e}_3^u = \hat{e}_1^u \times \underline{f}_2^u / |\hat{e}_1^u \times \underline{f}_2^u| \qquad\qquad (B19)$$

where, as in equation (B 17), the denominator is for the purpose of normalizing the result to a unit vector. Finally, $\hat{e}_2^u$ can be found directly from $\hat{e}_1^u$ and $\hat{e}_3^u$; i.e.,

$$\hat{e}_2{}^u = \hat{e}_3{}^u \times \hat{e}_1{}^u \qquad\qquad (B20)$$

Now the relation between $\underline{k}^u$ and $\underline{k}^d$ can be determined. This relation is found from the relations between wavenumber k and wavelength λ

$$k^u = 2\pi/\lambda^u \qquad\qquad k^d = 2\pi/\lambda^d \qquad\qquad (B21)$$

along with the value of $\underline{f}_3{}^u$ obtained by replacing $\underline{k}^d$ with $\Omega_j{}^d$ in equation (B11a) and by the knowledge that $\underline{k}^u$ and $\underline{k}^d$ are parallel to the vectors $\hat{e}_3{}^u$ and $\hat{e}_3{}^d$ respectively. Consider a vector $\lambda^d \hat{e}_3{}^d$ in the post-contraction fluid. If this vector begins on the crest of a wave of the turbulence wavevector component, it will reach just to the next crest since the vector has magnitude λ^d; see figure 6. In the pre-contraction fluid the vector begins and ends on the corresponding adjacent crests, but not necessarily along the shortest distance; i.e., the vector will not necessarily be along $\hat{e}_3{}^u$. If this upstream vector is denoted $\underline{h}_3{}^u$, then following the definitions in equations (B17) and (B18)

$$(h_3{}^u)_i = \lambda^d (f_3{}^u)_i = \lambda^d (e_3{}^d)_j \, (\partial x_i / \partial \xi_j) \qquad\qquad (B22)$$

The component of $\underline{h}_3{}^u$ in the direction of $\hat{e}_3{}^u$ must have a length λ^u from the above discussion. Thus,

$$\lambda^u = \underline{h}_3{}^u \cdot \hat{e}_3{}^u = \lambda^d \, (e_3{}^u)_i \, (e_3{}^d)_j \, (\partial x_i / \partial \xi_j) \qquad\qquad (B23)$$

From equation (B21)

$$k^d / k^u = (e_3{}^u)_i \, (e_3{}^d)_j \, (\partial x_i / \partial \xi_j) \qquad\qquad (B24)$$

The relations between the pre-contraction and post-contraction values of both wavenumber and velocity can be determined from the above relations. The procedure is first to find the three pre-contraction $\hat{e}^u$ vectors from the three post-contraction $\hat{e}^d$ vectors using equations (B17) through (B20). The ratio k^d / k^u can then be found from equation (B24). Finally, $\underline{Q}^u$ can be found from equation (B16).

Several of the vector operations in equation (B16) need not actually be carried out. The necessary operations have already been performed in deriving the $\hat{e}^u$ vectors. Thus, since $k_l{}^d$ and $Q_m{}^d$ are orthogonal,

$$k_l{}^d \, Q_m{}^d \, \epsilon_{lmn} = - (e_1{}^d)_n \, k^d \, Q^d \qquad\qquad (B25)$$

The vector $(e_1{}^d)_j \, \partial x_i / \partial \xi_j$ has already been calculated in equation (B17) and is the vector $\underline{f}_1{}^u$ parallel to $\hat{e}_1{}^u$. Thus equation (B16) can be written

$$Q_i{}^u(\underline{k}^u) = Q^d(\underline{k}^d) \, f_1{}^u \, \hat{e}_2{}^u \, k^d / k^u \qquad\qquad (B26)$$

A computer program was initially written using equation (B16). This was changed to the simplified version using equation (B26), and the programs were found to agree.

4. Comparison with Results of Ribner and Tucker

25

a. Wavenumber Relation

Ribner and Tucker[15] have performed this same analysis, but for the restricted case where the deformation tensor is diagonal. This is no restriction in principle since a rotation to principal coordinates can always be performed in which the deformation tensor is diagonal. In practice the present method may be simpler. The present results will be examined to verify that they reduce to those of Ribner and Tucker.

The deformation considered by Ribner and Tucker is

$$\left[\frac{\partial x_j}{\partial \xi_j}\right] = \begin{bmatrix} \ell_1^{-1} & 0 & 0 \\ 0 & \ell_2^{-1} & 0 \\ 0 & 0 & \ell_3^{-1} \end{bmatrix} \tag{B27}$$

The relation given between $\underline{k}^d$ and $\underline{k}^u$ is

$$\underline{k}^d = (k_1^u/\ell_1,\ k_2^u/\ell_2,\ k_3^u/\ell_3) \tag{B28}$$

This can be shown to follow from equations (B24) and (B27); i.e., multiplication of equation (B24) by k^d gives

$$k^{2d} = k_i^u k_j^d\, \partial x_i/\partial \xi_j = k_1^u k_1^d \ell_1^{-1} + k_2^u k_2^d \ell_2^{-1} + k_3^u k_3^d \ell_3^{-1} \tag{B29}$$

This will hold for all k values if

$$k_1^u \ell_1^{-1} = k_1^d \qquad\qquad k_2^u \ell_2^{-1} = k_2^d \qquad\qquad k_3^u \ell_3^{-1} = k_3^d \tag{B30}$$

Equation (B30) agree with equation (B28). Thus, the procedure for calculation of $\underline{k}^u$ from $\underline{k}^d$ presented here reduces to that of Ribner and Tucker for a diagonal deformation tensor.

b. Velocity Relation

Equation (B16) for the relation between pre-contraction and post-contraction velocities can similarly be reduced to the form given by Ribner and Tucker. Notation presents a minor problem in that the use of the Cartesian indices can be confusing. The notation used here is that a subscript in parentheses is a duplicate index and is not summed over unless the index appears twice elsewhere in the expression. Thus, $A_i\, B_{(i)}$ implies no summation over i, but the variable B has the same index as A. However, for $A_i\, B_i\, C_{(i)}$, summation over i is assumed with C in each term of the summation taking the same index as A and B.

Equation (B16) is rewritten into the form used by Ribner and Tucker relating the post-contraction velocity $\underline{Q}^d$ to the pre-contraction value $\underline{Q}^u$ (rather than vice versa as in equation (B16)). Then

$$Q_i^d(\underline{k}^d) = -\,(k_j^d/k^{2d})\, k_l^u\, Q_m^u(\underline{k}^u)\, \epsilon_{lmn}\, (\partial \xi_k/x_n)\, \epsilon_{ijk} \tag{B31}$$

Using the inverse of equation (B27) gives

$$Q_i^d(\underline{k}^d) = -(k_j^d/k^{2d})\, k_l^u\, Q_m^u(\underline{k}^u)\, \epsilon_{lmn}\, \epsilon_{ijn}\, \ell_{(n)} \tag{B32}$$

Now

$$\ell_1\, \ell_2\, \ell_3 = 1 \tag{B33}$$

for incompressible flow since the determinant of the deformation matrix must be 1 as discussed previously. Then since $\epsilon_{ijn} = 0$ unless $i \ne j \ne n$, equation (B32) can be written

$$Q_i^d(\underline{k}^d) = -(k_j^d/k^{2d})\, k_l^u\, Q_m^u(\underline{k}^u)\, \epsilon_{lmn}\, \epsilon_{ijn}\, [\ell_{(i)}\, \ell_{(j)}]^{-1} \tag{B34}$$

Using the relation

$$\epsilon_{lmn}\, \epsilon_{ijn} = \delta_{il}\, \delta_{jm} - \delta_{im}\, \delta_{jl} \tag{B35}$$

equation (B34) becomes

$$Q_i^d = (k_j^d/k^{2d})[\ell_{(i)}\, \ell_{(j)}]^{-1}(k_j^u\, Q_i^u - k_i^u\, Q_j^u) \tag{B36}$$

Introducing equation (B30)

$$Q_i^d = \frac{1}{\ell_{(i)}}\left[Q_i^u - \frac{k_j^u\, k_i^u}{\ell_{(j)}^2\, k^{2d}}\, Q_j^u \right] \tag{B37}$$

But this is exactly equation (13) of reference 15. Thus, the present result relating pre-contraction and post-contraction velocity reduces to the previously derived result of Ribner and Tucker for the case of a diagonal deformation tensor.
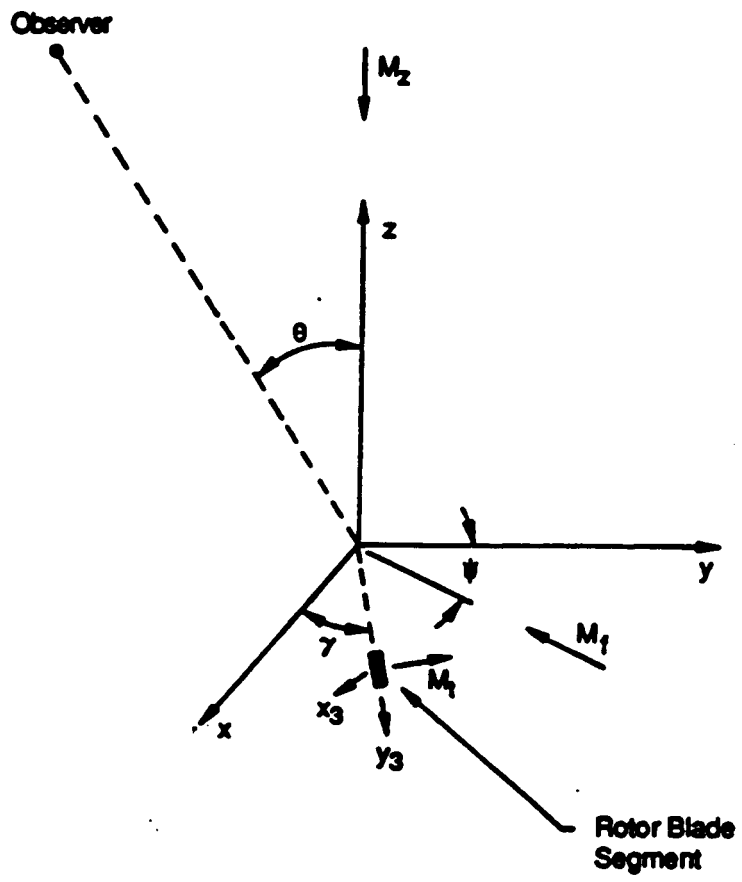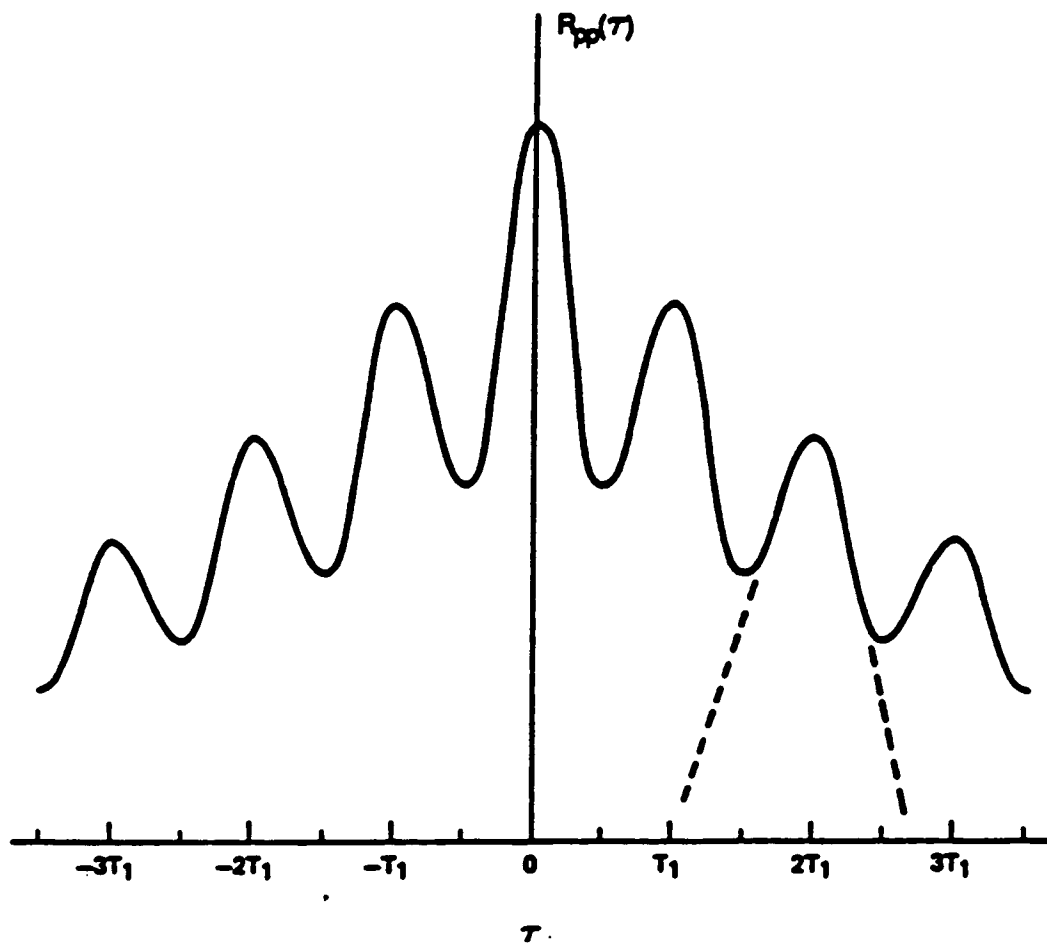
27

Figure 1: Geometry of rotor problem.

28

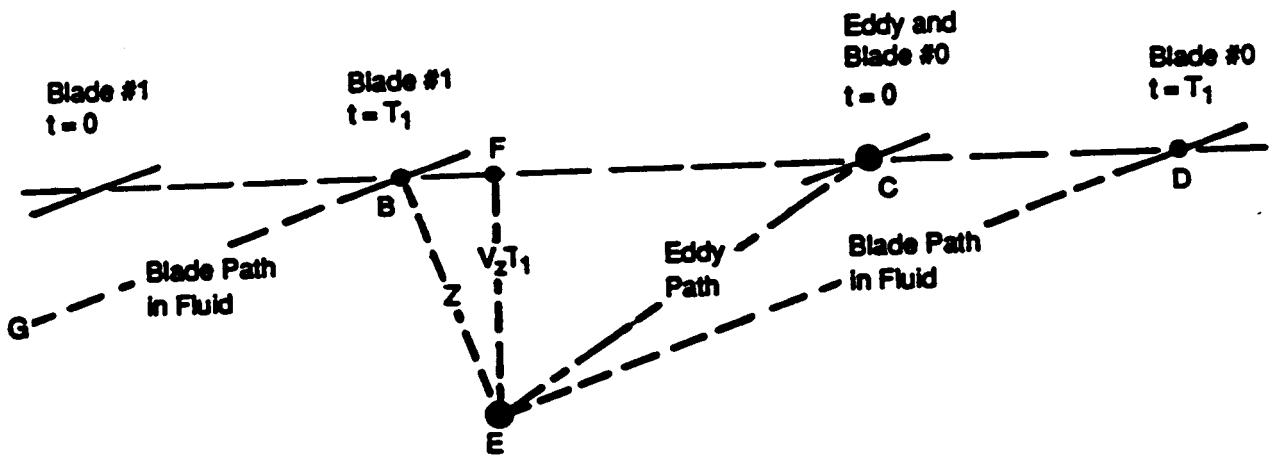Figure 2: Sample cross-correlation of far-field noise.
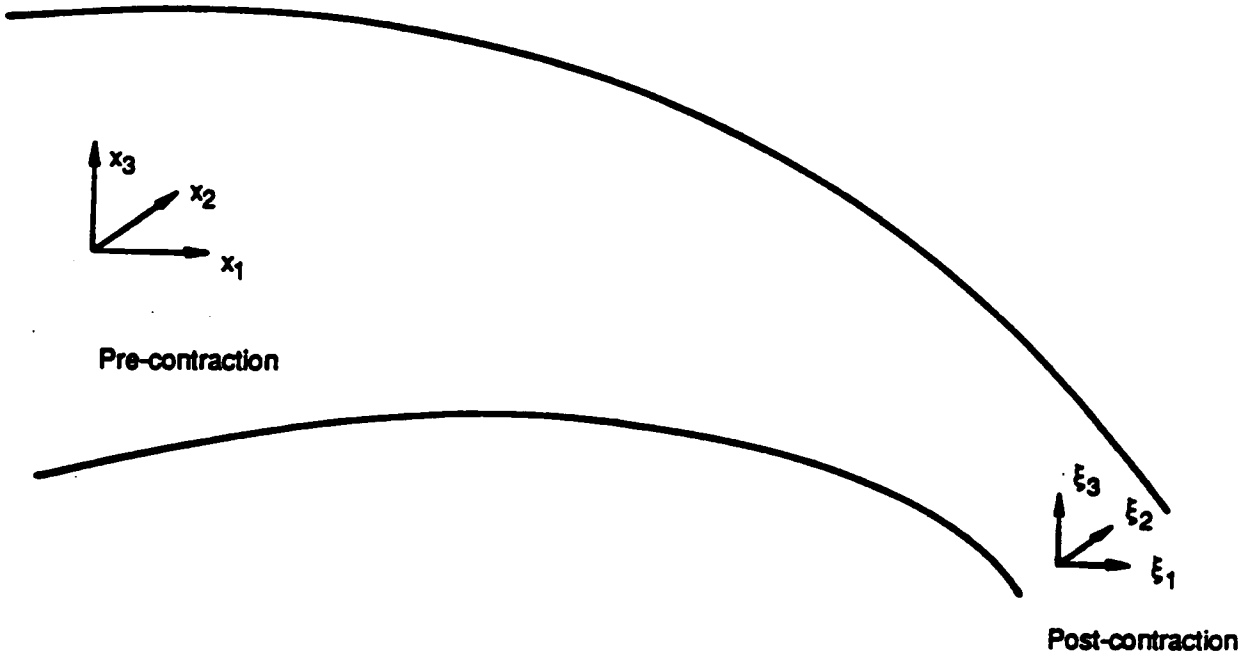
Figure 3: Kinematics of eddy cutting process.

Figure 4: Sketch of pre-contraction and post-contraction coordinate systems.
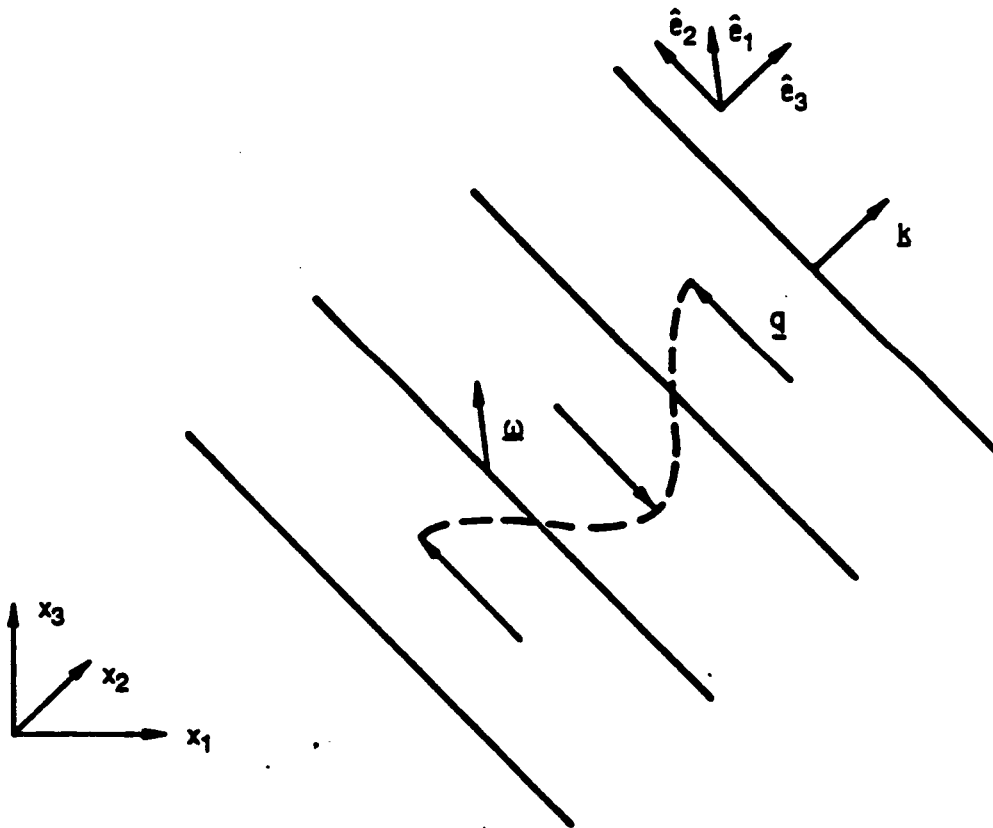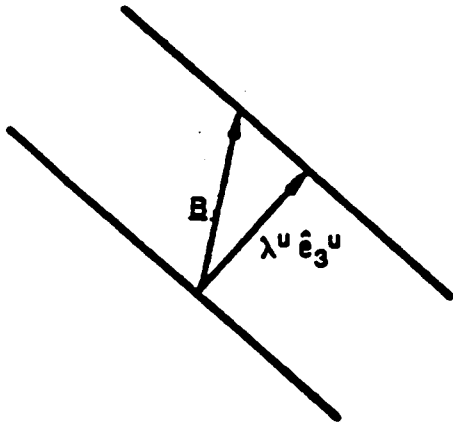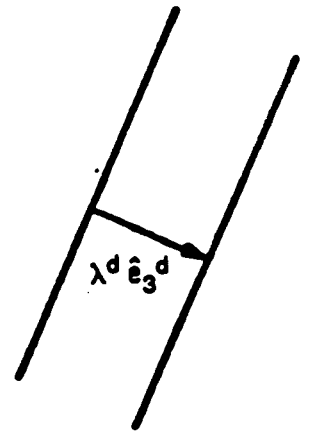
31

Figure 5: Sinusoidal velocity variation for a wavevector component of turbulence.

Pre-contraction
turbulence
Fourier
component

Post-contraction
turbulence
Fourier
component

$\underline{B}$

$\lambda^u \, \hat{e}_3{}^u$

$\lambda^d \, \hat{e}_3{}^d$

$\lambda^d \, \hat{e}_3{}^d$ transforms to a vector $\underline{B}$ using equation (B11).

λ^u is found from the relation $\lambda^u = \underline{B} \cdot \hat{e}_3{}^u$

Figure 6: Relation between pre-contraction and post-contraction wavevectors.

33

NASA
National Aeronautics and Space Administration

Report Documentation Page

1. Report No. NASA CR-181788	2. Government Accession No.	3. Recipient's Catalog No.

4. Title and Subtitle	5. Report Date
Noise Produced by Turbulent Flow Into a Rotor: Theory Manual for Noise Calculation	June 1989
	6. Performing Organization Code

7. Author(s)	8. Performing Organization Report No.
R. K. Amiet	
	10. Work Unit No. 505-63-51

9. Performing Organization Name and Address	11. Contract or Grant No.
United Technologies Research Center East Hartford, CT, 06108	NAS1-17763
	13. Type of Report and Period Covered

12. Sponsoring Agency Name and Address	Contractor Report
National Aeronautics and Space Administration Langley Research Center Hampton, VA 23665-5225	14. Sponsoring Agency Code

15. Supplementary Notes

Langley Technical Monitor: Thomas F. Brooks
Final Report

16. Abstract

An analysis is presented for the calculation of noise produced by turbulent flow into a helicopter rotor. The method is based on the analysis of Amiet for the sound produced by an airfoil moving in rectilinear motion through a turbulent flow field. The rectilinear motion results are used in a quasi-steady manner to calculate the instantaneous spectrum of the rotor noise at any given rotor position; the overall spectrum is then found by averaging the instantaneous spectrum over all rotor azimuth angles. Account is taken of the fact that the rotor spends different amounts of retarded time at different rotor positions. Blade to blade correlation is included in the analysis, leading to harmonics of blade passing frequency. The spectrum of the turbulence entering the rotor is calculated by applying rapid distortion theory to an isotropic turbulence spectrum, assuming that the turbulence is stretched as it is pulled into the rotor. The inputs to the program are obtained from the atmospheric turbulence model and mean flow distortion calculation, described in another volume of this set of reports. This study provides the analytical basis for a module which has been incorporated in NASA's ROTONET helicopter noise prediction program.

17. Key Words (Suggested by Author(s)). turbulence noise, rotor noise, narrow band noise	18. Distribution Statement Unclassified - Unlimited Subject Category 71

19. Security Classif. (of this report) Unclassified	20. Security Classif. (of this page) Unclassified	21. No. of pages 35	22. Price A03